Indian Journal of Radio & Space Physics
Vol. 30, October 2001, pp. 254-259

A model study of the atmospheric heating rates due to O_3, H_2O and O_2

M Lal

Equatorial Geophysical Research Laboratory, Indian Institute of Geomagnetism,
Krishnapuram, Maharajanagar, Tirunelveli 627 011

Received 26 June 2000; revised 30 March 2001; accepted 14 June 2001

The height distribution of solar heating rate due to ozone, water vapour and oxygen molecule from ground to 100 km altitude has been examined in this study. The cooling rate due to infrared emission of CO_2, O_3 and water vapour molecules has also been studied for middle atmospheric region. The heating and cooling rates have been calculated for midlatitude and equinox condition. The diurnal variation of net radiative temperature change in tropospheric and stratospheric region causes generation of waves, which propagate in the mesospheric region and affects the climatology of the upper atmosphere. The heating rate due to water vapour is found to be important in the troposphere, ozone heating is significant in the stratosphere, and oxygen heating rate is found to be important in the mesospheric region. The maximum ozone heating rate in the stratospheric region is found to be ~ 15 K/day. The cooling rate due to CO_2 is very significant in the stratospheric region and is found to be about –12 K/day. The net radiative temperature change due to heating and cooling has been obtained to be similar to the atmospheric temperature profile.

1 Introduction

The ultraviolet and visible solar radiation, absorbed by atmospheric ozone, is the principal energy source of large-scale dynamical phenomena in the middle atmosphere. The total diabatic heating in the middle atmosphere is frequently governed by numerous sources including the heat generated through absorption of solar ultraviolet radiation by ozone in the Hartley band and by molecular oxygen in the Schuman-Runge band, Schuman-Runge continuum, Hertzberg band and at Lyman–α wavelengths. The visible wavelength radiation are mainly absorbed by the ozone in the Huggins and Chappuis band at lower stratosphere and tropospheric region. The near IR radiation is absorbed by water vapour in the tropospheric region. Thus the oxygen in mesosphere, ozone in stratosphere and water vapour in troposphere are the major constituents responsible for solar heating. The molecules such as CO_2, H_2O and O_3 emit longwave radiation in the atmosphere and causes cooling. The maximum cooling due to H_2O is in the tropospheric region. The maximum cooling due to O_3 is in the stratospheric region, but the magnitude of cooling is very less compared to that due to CO_2. Therefore, the maximum cooling in the middle atmosphere occurs due to CO_2. The net radiative temperature change due to heating and cooling causes large-scale dynamical phenomena in the atmosphere; among them are the atmospheric tides[1,2] and the zonal mean circulation in the middle atmosphere[3-9]. In case of atmospheric tides, the temporal variations of ozone heating are mainly due to the rotation of the earth, while in the case of zonal mean circulation in the middle atmosphere, the variations are primarily caused by the change of the earth-sun geometry, particularly, the change of solar declination. In reality, these two variations are superposed on each other. Temporal variation of tropospheric water vapour heating rates, stratospheric ozone heating rates in different bands, energy absorbed by ozone and water vapour for different amount of these species, and total heating rate from ground to 100 km due to H_2O, O_3, and O_2 have been calculated in the present work. The cooling rate has also been evaluated for the middle atmospheric region. The cooling rate has been calculated, separately, for CO_2, H_2O and O_3 molecules.

However, the observations of the middle atmosphere can be used to calculate the location and strength of the radiative sources and sinks. Such calculations are important, because radiative heating is the only important diabatic term for most of the middle atmosphere and can be thought of as providing the forcing for the diabatic circulation[10,11]. The diabatic circulation is the major component of the residual mean circulation, which plays an important role in the transport of the chemical and dynamical quantities[12] of the lower and middle atmosphere.

2 Formulation of heating rate due to water vapour and ozone absorption

If the downward and upward energy fluxes are $F\downarrow$ (z) and $F\uparrow$ (z) for the solar flux incident on the height z, the heating rate per unit mass of the atmosphere is given by

$$J_a = (1/\rho).d/dz\ (F\downarrow - F\uparrow) \quad \ldots (1)$$

where, ρ is the air density[13,14]. These energy flux vary for different amount of absorber and can be expressed in terms of absorption (A) as

$$F\downarrow = \cos\chi\ .\ S_o.\ (1-A) \quad \ldots (2)$$

where, S_o is the solar flux at the top of the atmosphere and χ the solar zenith angle.

Similar to the downward flux, Groves[13,14] define the absorption of the upward flux A' by

$$F\uparrow = R\ (\cos\chi)S_o\ (1-A') \quad \ldots (3)$$

where, R is the albedo of the reflecting surface. An effective optical path mu' is then defined by

$$A\ (mu') = A'$$

and A' is obtained by adopting an approximate expression for y', which is as follows:

$$y' = M.w_t + 5/3\ (w_t - w) \quad \ldots (4)$$

where, w_t is the total water vapour amount above the reflecting surface and 5/3 is an average magnification factor for diffuse radiation.

By substituting the values of $F\downarrow$ (z) and $F\uparrow$ (z) from Eqs (2) and (3) to Eq. (1), the heating rate per unit mass can be derived as

$$J_{\alpha 1} = q\eta^{\circ}(\cos\chi)S_o[MA_1(y) + (5/3)RA_1(y')] \quad \ldots (5)$$

where,

$$A_1 = dA/dy = 2.9[(0.635+0.365.Y)/(Y^{0.635} + 5.925\ y)^2\ .\ Y^{0.365}]\ \ cm^2.g^{-1}$$

where, $Y = (1+141.5\ y)$

The heating rate in K/day can be obtained by the following equation

$J = (J_{\alpha 1}/\ C_p)\ (2.06\ 10^4)$ K/day

where, $Cp = 0.24$ cal.$gm^{-1}.k^{-1}$

The ozone heating rate (Q) has been derived by Brasseur and Solomon[15] and is as follows:

$$Q = \partial T/\partial t = (1/\rho.C_p).n(O_3)\ f_v\ \sigma(O_3)\ F_{s,v}\ dv \quad \ldots (6)$$

where, $n(O_3)$ is the ozone density, ρ air density, $\sigma(O_3)$ the absorption coefficient, $F_{s,v}$ the solar flux at the height z and v the wavenumber.

3 Input parameters

Table 1 presents calculated mixing ratio, tempera-

Table 1—Profiles of the temperature T, air density {[M]}, pressure (P), H_2O mixing ratio, O_3 mixing ratio, O_2 column and O_3 column variation from 0 to 100 km altitude

Altitude km	T (K)	[M] cm^{-3}	P mbar	H_2O	O_3	Ozone column cm^{-2}	O_2 column cm^{-2}
0	288.8	2.5(19)	1013.0	1.4(-2)	3.0(-8)	9.5(18)	4.8(24)
5	259.3	1.5(19)	542.0	1.0(-3)	5.1(-8)	9.1(18)	2.5(24)
10	229.7	8.5(18)	269.0	3.6(-5)	8.9(-8)	8.7(18)	1.2(24)
15	212.6	4.2(18)	122.0	2.9(-6)	5.2(-7)	8.1(18)	5.5(23)
20	215.5	1.8(18)	55.0	3.3(-6)	2.7(-6)	6.3(18)	2.5(23)
25	218.6	8.3(17)	25.0	3.9(-6)	5.9(-6)	3.7(18)	1.2(23)
30	223.7	3.7(17)	11.5	4.4(-6)	8.3(-6)	1.7(18)	5.6(22)
35	235.1	1.7(17)	5.4	4.8(-6)	8.0(-6)	5.6(17)	2.8(22)
40	249.9	7.7(16)	2.7	5.2(-6)	5.1(-6)	1.7(17)	1.4(22)
45	266.1	3.8(16)	1.4	5.4(-6)	3.3(-6)	5.8(16)	7.5(21)
50	271.0	2.0(16)	0.73	5.5(-6)	2.1(-6)	2.0(16)	4.1(21)
55	265.3	1.1(16)	0.38	5.6(-6)	1.4(-6)	7.6(15)	2.1(21)
60	253.7	5.7(15)	0.20	5.6(-6)	1.0(-6)	2.8(15)	1.0(21)
65	237.0	3.0(15)	0.10	5.7(-6)	8.6(-7)	9.5(14)	4.7(20)
70	220.2	1.5(15)	0.046	5.7(-6)	4.0(-7)	3.1(14)	2.2(20)
75	203.4	7.4(14)	0.021	5.7(-6)	1.8(-7)	1.6(14)	1.0(20)
80	186.7	3.4(14)	0.0089	5.6(-6)	2.7(-7)	1.1(14)	4.2(19)
85	170.0	2.3(14)	0.0055	3.4(-6)	7.4(-7)	6.0(13)	2.4(19)
90	177.5	1.1(14)	0.0027	2.1(-6)	3.6(-7)	1.2(13)	1.2(19)
95	193.0	4.9(13)	0.0013	1.2(-6)	1.1(-7)	2.6(12)	5.7(18)
100	209.2	2.2(13)	0.00064	7.2(-7)	1.1(-7)	1.0(12)	2.9(18)

Note: 2.2(13) can be read as 2.2^{+13}; 7.2(-7) can be read as 7.2^{-7} and so on.

ture, air density, oxygen and ozone column content profiles obtained by a one-dimensional radiative convective photochemical model for midlatitude at equinox[15]. The mixing ratio indicated here is consistent with the photochemical rate expressions given by Brassuer and Solomon[15]. These values should only be considered as estimates, based on presently accepted photochemistry.

4 Results and discussion

Figure 1(A) shows the log of specific humidity variation with respect to altitude. This has been derived by using water vapour mixing ratio profile taken from Brasseur and Solomon[15] for midlatitude and equinox. If r is the water vapour mixing ratio and q is the specific humidity, then

$$q = r/(1+r)$$
or, $q \cong r$

because, vapour exist only in trace abundance. Hence, to a good approximation, q and r can be used interchangeably[16]. Figure 1(B) shows the log effective water vapour amount as a function of altitude. It is observed from Fig. 1(B) that the log effective water vapour decreases almost exponentially with height. The solar energy absorbed by effective water vapour amount varies with altitude. Using effective water vapour profile, absorbed solar energy by water vapour below 30 km has been calculated.

Figure 2 shows the variation of water vapour amount (in g.cm^{-2}) as a function of absorbed energy (erg.cm^{-2}.s^{-1}). It is noticed that the water vapour amount is in phase with the absorbed solar energy for

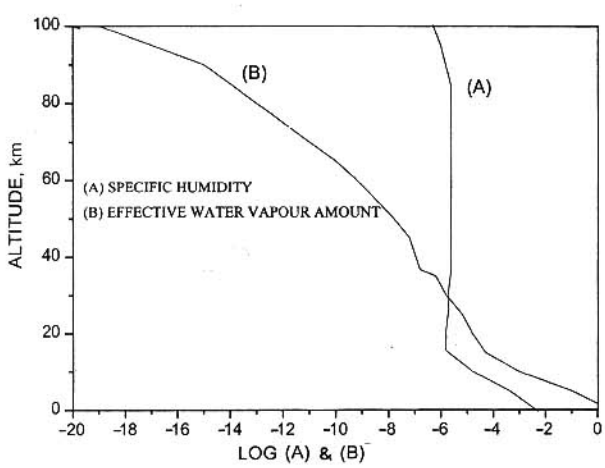

Fig. 1—(A) Curve showing the log variation of specific humidity for different altitude and (B) the log effective water vapour amount for different altitude

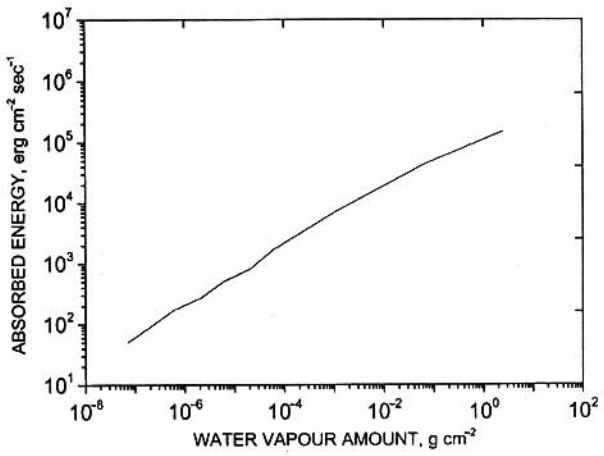

Fig. 2—Variation of water vapour amount (in g.cm^{-2}) for different absorbed energy (erg.cm^{-2}.s^{-1})

troposphere and lower stratosphere. The absorbed energy variation for different amount of water vapour has also been calculated by Howard *et al.*[17,18] for different spectral region between 0.945 and 6.3 micron. The total absorbed energy versus water vapour amount calculated by Howard *et al.*[17,18] and the present calculated energy values for lower values of water vapour amount are found to be similar. On the other hand, while the tropospheric values showed saturation at about 10^2 g.cm^{-2} of water vapour, the present calculated energy values for larger amount of water vapour does not show any significant saturation value. This difference may be due to the different solar flux, and also the attenuation due to scattering has not been taken into account.

Figure 3 shows the variation of ozone column density (in cm-atm NTP) with absorbed energy (erg.cm^{-2}.s^{-1}) for Hartley and Huggins bands. These values have been calculated for 0° solar zenith angle, midlatitude and equinox condition. It can be seen that the absorbed energy in Huggins band (300-370 nm) increases linearly with the increase in ozone column density. In the case of Hartely band (200-300 nm), absorbed energy increases linearly as the ozone column density increases up to 10^{-2} cm-atm NTP. Above ozone column density of 10^{-2} cm-atm NTP, absorbed energy approaches a constant value for Hartly band. This may be due to the limited amount of UV radiation available in the stratosphere. On the other hand, the solar flux above 300 nm wavelength region reaches to the earth's surface. Therefore, for getting the saturated values of absorbed energy, it is essential to have the ozone values much larger than those existing in the troposphere. Figure 3 also shows the

total absorbed energy due to ozone between 200 and 370 nm wavelength region. The total absorbed energy increases linearly up to about 10^{-2} cm-atm NTP of ozone and then becomes almost constant for higher values of ozone column amount. Similar calculation has also been done by Shimazaki[19]. He found that the solar energy is absorbed mainly in the Hartely band for ozone column density of less than about 0.1 cm-atm NTP. The present values are found to be in agreement with those of Shimazaki[19].

Figure 4 shows the height variation of the heating rate due to ozone absorption by Hartely, Huggins and Chappuis bands, representing the midlatitude equinox. The heating rate is expressed in K/day. The maximum ozone heating occurs mainly in the Hartely band and above about 30 km altitude region. The heating due to Hartely band shows another maxima in the mesospheric region. This may be due to the secondary peak of ozone density in the mesospheric region. The lower heating is mainly due to Chappuis band. The heating due to ozone in the Chappuis band has the maximum value of about 2 K/day. In the transition region, the heating due to Huggins band is important. This is mainly between 30 and 50 km altitude region. The maximum heating due to Huggins band is at about 35 km altitude. Similar to the Hartley band, Huggins band also shows secondary increasing trend in the mesospheric region, but the magnitude is much less than the Hartely band. Thus, the maximum heating due to ozone occurs mostly in the stratospheric region. The mesospheric region also shows heating due to ozone, but the magnitude of heating in stratosphere is very large compared to the mesosphere.

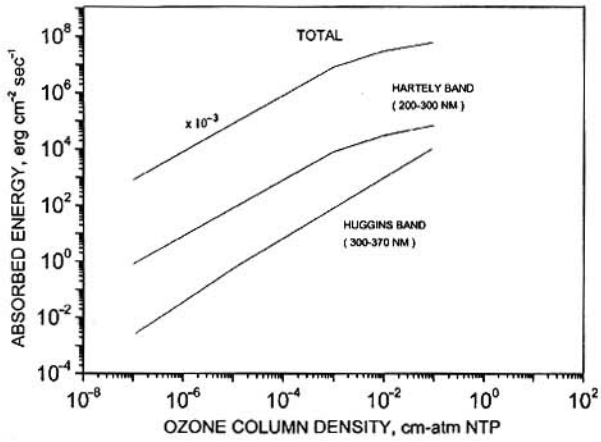

Fig. 3—Curves showing the variation of ozone column density (in cm-atm NTP) for different absorbed energy (erg.cm^{-2}.s^{-1})

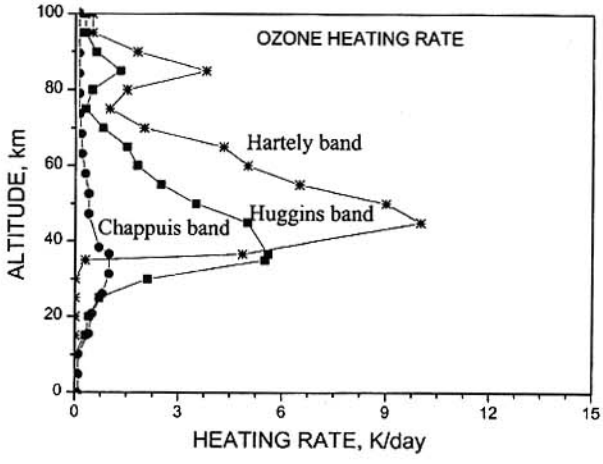

Fig. 4—Height variations of the heating rate due to ozone absorption at Hartely, Huggins and Chappuis bands, representing the midlatitude equinox

Figure 5 shows the midlatitude heating profile of water vapour for 0°, 30° and 60° solar zenith angles. The water vapour heating rates on the surface are 1.6, 1.2 and 0.4 K/day, respectively. This heating rate decreases exponentially with increase in altitude. This decreasing pattern may be due to the decrease in water vapour density with height in troposphere. The stratospheric heating rate due to water vapour calculated in the present study found to be very small and can be considered as insignificant in the middle atmosphere.

Figure 6 shows the midlatitude cooling profile of CO_2, H_2O and O_3. It also shows that the CO_2 cooling rate is very much significant in the stratospheric region. The maximum cooling rate is found to be –10 K/day at the stratopause. The ozone cooling maxima has also been found in the stratospheric region and its magnitude is about –2 K/day. The maximum cooling

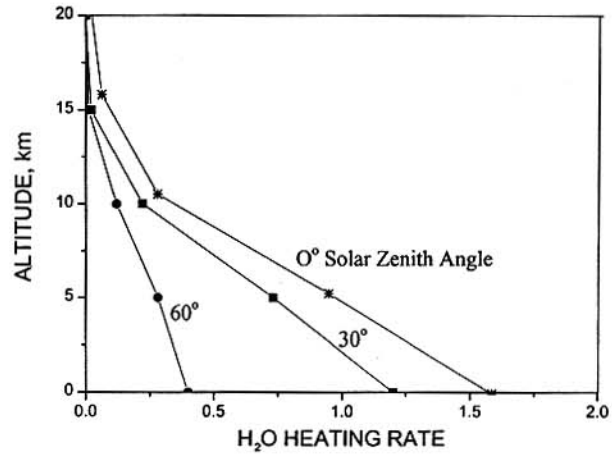

Fig. 5—Curves showing the midlatitude heating profile of water vapour for 0°, 30° and 60° solar zenith angles

due to water vapour is found in the upper layer of tropospheric region and its value is similar to ozone maxima. The tropospheric water vapour mixing ratio and CO_2 mixing ratio are highly variable. Therefore, the calculations are done for comparitavely stable region.

Figure 7 shows the total heating and cooling rate obtained from ground to 100 km altitude region. The present work has been compared with the heating and cooling rate derived by London[20]. The present model is found to be similar to that of London[20]. The heating as well as cooling shows maxima near the stratopause. The heating is found to be significant due to water vapour in troposphere, ozone in stratosphere and oxygen in the upper mesospheric region. The cooling due to water vapour is found to be significant at the upper layer of troposphere, due to ozone in the stratosphere with less magnitude and due to CO_2 in the stratosphere with maximum magnitude.

The net radiative temperature change due to heating and cooling rate obtained is shown in Fig. 8. Figure 8 shows that the net radiative change in the tropospheric region is mainly cooling of the atmosphere and stratospheric region is found to be the place of net increase in temperature. The lower mesospheric region shows the cooling band and upper mesospheric region is found to be the place of net increase in temperature. The net radiative temperature change in the present study is almost similar to the middle atmospheric temperature profile.

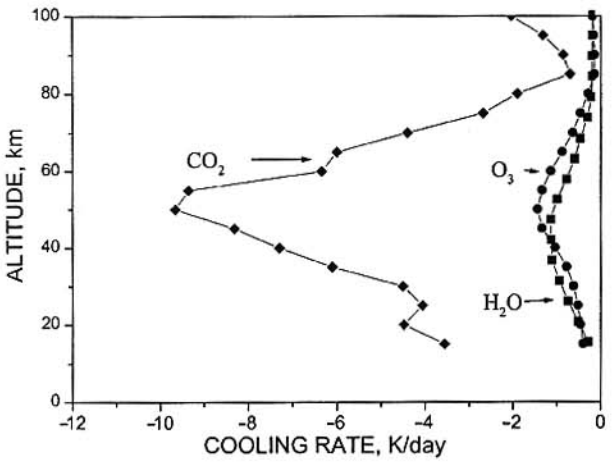

Fig. 6—Curves showing the midlatitude cooling profile of CO_2, H_2O, and O_3

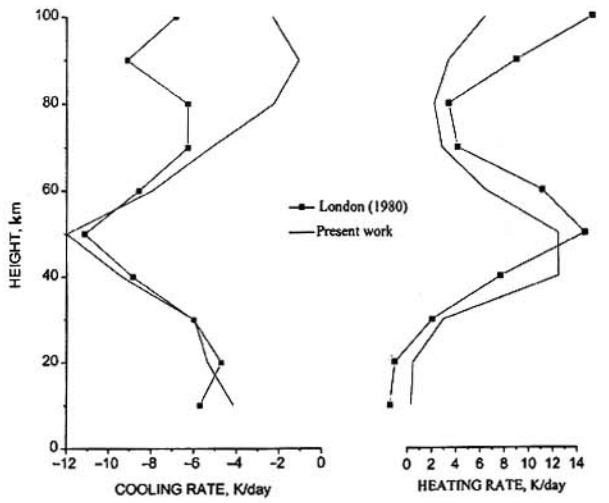

Fig. 7—Vertical distribution of solar short wave heating rates by O_3, O_2, H_2O and terrestrial long wave cooling rates by CO_2, O_3, and H_2O

5 Summary

In this model study, the height distribution of solar heating and cooling rate due to ozone, water vapour, oxygen and CO_2 from ground to 100 km altitude, has been examined. This heating and cooling rate has been calculated for midlatitude and equinox condition. Heating is calculated by assuming the average of the effective albedo to be 0.25. The effective albedo takes into account the combined effect of reflection from clouds and the ground. The heating rate due to water vapour is found to be important in the troposphere. The ozone heating is significant in stratosphere with its value ~ 15 K/day. A secondary peak of the ozone heating rate is found in the mesospheric region. This may be due to the secondary peak of ozone density. The calculation has also been done for oxygen heating rate in the mesospheric and lower ionospheric region. Heating due to oxygen is found to

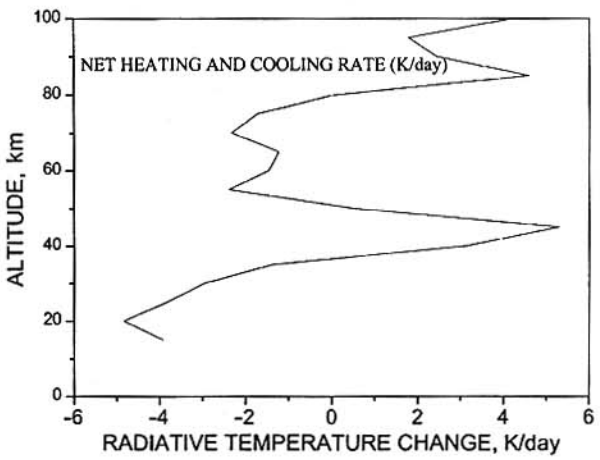

Fig. 8—Curve showing the net heating and cooling rates due to CO_2, O_3, NO_2 and H_2O for the midlatitude and equinox condition

be increasing with altitude approximately exponentially. Calculations are also made for the cooling rate due to CO_2, H_2O and O_3 molecules for the middle atmospheric region. The cooling rate due to CO_2 is significant in the stratospheric region and maximum cooling is found to be –10 K/day. The cooling due to O_3 is maximum in stratosphere and H_2O cooling is found to be in the tropospheric region. The net cooling is significant in the stratospheric region and the present calculated values are found to be similar to those obtained by London[20]. The net radiative temperature change due to heating and cooling obtained in the present work is found to be similar to the atmospheric temperature profiles.

Acknowledgement

The author is thankful to Prof. R Rajaram, Indian Institute of Geomagnetism, Mumbai, for his valuable suggestion. This work was supported by Department of Science and Technology, India.

References

1 Chapman D & Lindzen R S, *Atmospheric Tides* (D Reidel Publishing Co., Dordrecht, Holland) 1970, p. 200.
2 Hong S & Wang P H, *Bull Geophys (Taiwan)*, 19 (1980) 56.
3 Murgatroyd R J & Singleton F, *Q J R Meteorol Soc (UK)*, 87 (1961) 125.
4 Leovy C B, *J Atmos Sci (USA)*, 21 (1964) 327.
5 Harwood R S & Pyle J A, *Q J R Meteorol Soc (UK)*, 101 (1975) 723.
6 Schoeberl M R & Strobel D F, *J Atmos Sci (USA)*, 35 (1978) 577.
7 Crane A I, Haigh J C, Pyle J A & Rogers C F, *Pure & Appl Geophys (USA)*, 118 (1980) 307.
8 Holton J R & Wehrbein W M, *Pure & Appl Geophys (USA)*, 118 (1980) 284.
9 Holton J R & Wehrbein W M, *J Atmos Sci (USA)*, 37 (1980) 1968.
10 Dunkerton T, *J Atmos Sci (USA)*, 35 (1978) 2325.
11 Wang P H, Hong S S, Wu M F & Deepak A, *J Atmos Sci (USA)*, 39 (1982) 1398.
12 Gille J C, Lyjk L V & Smith A K, *J Atmos Sci (USA)*, 44 (1987) 256.
13 Groves G V, *J Atmos & Terr Phys (U K)*, 44 (1982) 281.
14 Groves G V, *J Atmos & Terrs Phys (U K)*, 44 (1982) 111.
15 Brasseur G & Solomon S, *Aeronomy of the middle atmosphere* (D Reidel Publishing Co., Dordrecht, Holland), 1986.
16 Salby M I, *Fundamentals of atmospheric physics* (Academic press, New York), 1996.
17 Howard J N, Burch D F & Williams D, *J Opt Soc Am (USA)*, 46 (1956) 237.
18 Howard J N, Burch D F & Williams D, *J Opt Soc Am (USA)*, 46 (1956) 242
19 Shimazaki T, *Minor constituents in the middle atmosphere* (D Reidel Publishing Co., Dordrecht, Holland), 1985, p.200.
20 London J, *Proceedings of the Nato Advanced Institute on Atmospheric Ozone (Portugal)*, U S Dept of Transportation, FAA – Washington, DC, USA- No. FAA-EE-80-20, 1980.